# Quantifying Eddy Feedbacks and Forcings in the Tropospheric Response to Stratospheric Sudden Warmings

PETER HITCHCOCK

*Department of Applied Mathematics and Theoretical Physics, University of Cambridge, Cambridge, United Kingdom*

ISLA R. SIMPSON

*Climate and Global Dynamics Laboratory, National Center for Atmospheric Research, Boulder, Colorado*

(Manuscript received 15 February 2016, in final form 28 May 2016)

ABSTRACT

The equatorward shift of the zonal-mean midlatitude tropospheric jet following a stratospheric sudden warming in a comprehensive stratosphere-resolving model is found to be well quantified by the simple model of tropospheric eddy feedbacks proposed by Lorenz and Hartmann. This permits a decomposition of the shift into a component driven by the stratospheric anomalies and a component driven by tropospheric feedbacks.

This is done by extending the simple model to include three effective forcing mechanisms by which the stratosphere may influence the tropospheric jet. These include 1) the zonally symmetric adjustments associated with the mean meridional circulation and the direct influence of the stratospheric anomalies on 2) the tropospheric synoptic-scale or 3) the tropospheric planetary-scale eddies. Although the anomalous tropospheric winds are primarily maintained against surface friction by the synoptic-scale eddies, this response can be entirely attributed to the eddy feedback term. The response of the planetary-scale eddies, in contrast, can be directly attributed to the stratosphere. The zonally symmetric tropospheric circulation associated with downward control is found to play little role in driving the tropospheric response.

The prospects of applying this methodology to reanalysis data are also considered, but statistical limitations and the relatively weak projection of the vertically integrated composite wind anomalies onto the leading EOF preclude any conclusions from being drawn.

## 1. Introduction

Following the landmark paper of Baldwin and Dunkerton (2001), the equatorward shift of the zonally averaged, tropospheric, midlatitude jet following stratospheric sudden warmings has now been well established in the observational record (Limpasuvan et al. 2004) and in a wide variety of models of varying degrees of complexity (Yoden et al. 1999; Polvani and Kushner 2002; Gerber et al. 2010; Hitchcock and Simpson 2014, hereafter HS). A number of dynamical mechanisms have been proposed to explain this shift, but it has proven difficult to convincingly distinguish between or falsify these mechanisms. This is in part because of the strongly coupled nature of the system but is also a result of statistical difficulties due to both the relatively short observational record of the complete coupled stratosphere–troposphere system and the large interevent variability inherent to stratospheric sudden warmings. There is considerable interest in exploiting the enhanced skill in seasonal forecasts associated with these stratospheric events (Sigmond et al. 2013), so improving the dynamical understanding of the relevant processes has significant practical consequences.

Some progress has been made. There is, for instance, considerable evidence that changes in the synoptic-scale eddies play a central role in the tropospheric response. While the dynamical and radiative forcing associated with the event in the stratosphere are expected to produce a barotropic near-surface response, which is further amplified by the diabatic processes responsible

*Corresponding author address*: Peter Hitchcock, Dept. of Applied Mathematics and Theoretical Physics, Centre for Mathematical Sciences, Wilberforce Road, Cambridge CB3 0WA, United Kingdom.
E-mail: aph42@cam.ac.uk

DOI: 10.1175/JAS-D-16-0056.1

for downward control (Haynes et al. 1991), efforts to quantify this effect have found it inadequate to describe the full tropospheric response (e.g., Charlton et al. 2005). The response found by Thompson et al. (2006), for instance, was only able to explain the zonal-mean zonal wind changes at high latitudes, and not the bulk of the equatorward shift. Moreover, momentum fluxes associated with synoptic-scale eddies have been implicated in observational composites (Limpasuvan et al. 2004) and have been shown to be required to explain the tropospheric response in simplified models (Kushner and Polvani 2004; Song and Robinson 2004).

However, it well known that the synoptic-scale eddies respond strongly to changes in the tropospheric jet itself (Robinson 2000, and references therein), raising the difficult question as to what extent the change in eddies is responsible for the shift in the jet and to what extent the shift of the jet is responsible for the change in eddies. One manifestation of this feedback between the eddies and the jet is in the typical persistence of latitudinal shifts of the jet, which has been argued to be longer than it would be in the absence of these interactions (Robinson 1996; Lorenz and Hartmann 2001, hereafter LH01, 2003, hereafter LH03).

There is strong evidence that the same processes responsible for this persistence are also playing a role in the response to a variety of forcings in the climate system, including those arising from the stratosphere (Kidston et al. 2015). The large shifts in the tropospheric jets found by Polvani and Kushner (2002) and Kushner and Polvani (2004) in response to perturbations of the stratospheric vortex were shown by Chan and Plumb (2009) to be closely associated with extremely persistent variability in the tropospheric jets particular to the configuration of the dry dynamical core they used; when the character of the jet was modified such that this persistence was reduced, the response to the stratospheric perturbation was correspondingly weakened. Similar sensitivities of the forced response to the underlying variability of the tropospheric jet have been found by Simpson et al. (2010) and Garfinkel et al. (2013). The hypothesis that these internal feedbacks are a general feature of the forced response of the extratropical troposphere has the appealing merit of explaining why many different phenomena appear to drive responses with similar structures (Kidston et al. 2015).

Indeed the connection between the persistence of the tropospheric variability and the amplitude of the forced response is expected on general grounds as a consequence of the fluctuation–dissipation theorem (Leith 1975). This suggests that, all else being equal, the magnitude of the forced response should scale with the persistence time scale of internally produced fluctuations. This has been shown to have some explanatory power in a number of related contexts (Chan and Plumb 2009; Simpson et al. 2010; Kidston and Gerber 2010; Garfinkel et al. 2013). However, decorrelation time scales have been shown to be significantly influenced by variability external to the jet (Keeley et al. 2009; Simpson et al. 2011) and in some cases have been found to be a poor predictor of the magnitude of the tropospheric response (Hitchcock et al. 2013b; Simpson and Polvani 2016). These difficulties do not imply that the time scale is irrelevant, since, for instance, the response is also predicted by the fluctuation–dissipation theorem to depend on the projection of the relevant external forcing onto the structure of the mode of variability. More work is needed to fully understand the relationship between decorrelation time scales and feedback processes relevant for both the natural variability and forced responses.

While the tropospheric eddy feedback is almost certainly playing a central role in amplifying the tropospheric response to sudden warmings, it is nonetheless clear that there must be some stratospheric influence on the combined tropospheric jet–eddy system; otherwise, the jet would simply continue to fluctuate about its climatological state. One natural possibility, considered explicitly by Song and Robinson (2004), is that this influence is the direct, downward control response to the stratospheric forcing, which is then amplified by the tropospheric eddy feedbacks. A second possibility is that the anomalous stratospheric state is directly influencing the synoptic-scale eddies, either through modifying their growth rates (Tanaka and Tokinaga 2002; Wittman et al. 2007; Smy and Scott 2009) or by modifying how they propagate and break in the upper troposphere (Simpson et al. 2009). A third possibility is that the stratospheric state is influencing the planetary-scale eddies directly; this should be distinguished from the potential influence on the synoptic-scale eddies, given the different sources and propagation characteristics of planetary-scale waves. This was also considered by Song and Robinson (2004), who found that the tropospheric response was significantly modulated when they artificially damped the planetary-scale eddies in the stratosphere. Evidence for this pathway has recently been demonstrated in a set of dry dynamical core experiments (Smith and Scott 2016). This possibility was also raised in a broader context by DeWeaver and Nigam (2000; see also references therein).

An essential step forward in this problem is thus to be able to clearly separate the ''external'' stratospheric influence from the ''internal'' tropospheric feedbacks so that the two aspects can be identified and studied in isolation. The approach adopted here is to quantify the tropospheric feedback explicitly so that it can be removed diagnostically from the response. This is done

in the context of the vertically integrated tropospheric angular momentum budget and follows the analysis of LH01 and LH03, who quantified the tropospheric eddy feedback using an extremely simple parameterization of the vertically integrated eddy momentum flux convergence.

This analysis is applied to a set of recent integrations of the Canadian Middle Atmosphere Model (CMAM), a comprehensive stratosphere-resolving model, in which a large ensemble of tropospheric responses to, effectively, a single realization of a stratospheric event have been produced through a zonally symmetric nudging technique (HS). It will be shown that this simple parameterization can successfully describe the response of the zonal-mean tropospheric jet to stratospheric sudden warmings, both in the nudged ensemble and in composites of events produced by the free-running integration. In both cases the analysis clearly indicates that the influence of the stratosphere on the planetary-scale eddies in the troposphere is the key mechanism influencing the jet, while the direct influence of the stratosphere on the synoptic-scale eddies and the balanced, downward control response are relatively unimportant.

We also consider the application of this approach to the European Centre for Medium-Range Weather Forecasting interim reanalysis (ERA-Interim) dataset (Dee et al. 2011). However, a number of difficulties arise. First, the large intrinsic variability of the tropospheric eddy momentum flux convergences and the relatively few, well-observed stratospheric events pose significant statistical difficulties. Second, the composited vertically integrated zonal-mean zonal wind anomalies do not project nearly as dominantly onto the leading mode of internal variability as is the case in the CMAM integrations. These facts, demonstrated in the appendix, preclude the direct application of this methodology to the reanalysis.

The rest of the paper is structured as follows. Details of the nudging experiments are briefly reviewed in section 2, although readers are referred to HS for full details. Section 3 presents review of the formulation of the simple model of LH01 and LH03 and describes a set of simple extensions of this model to identify and quantify the possible stratospheric influences. The parameters of the Lorenz and Hartmann (LH) model are also fit to the internal variability of the CMAM integrations. The extensions are then each evaluated in turn in section 4. Finally, the main conclusions and a discussion of their implications are given in section 5.

## 2. Model, data, and event definitions

### a. Comprehensive model experiments

Three sets of integrations of CMAM are analyzed here. Details of the model numerics and physical parameterizations can be found in Scinocca et al. (2008). A brief summary of the numerical experiments is given in this section; a more complete discussion of the runs can be found in HS, while a theoretical discussion of the impacts of the nudging is given by Hitchcock and Haynes (2014). The first integration, referred to here as FREE, is a 100-yr, time-slice integration with climatologically specified ozone, sea surface temperatures, and sea ice concentrations. The integration does not produce a quasi-biennial oscillation, nor is one imposed. The second, referred to as CTRL, is another 100-yr, time-slice integration with the same boundary conditions, in which the zonally symmetric component of the winds and temperatures in the stratosphere are relaxed toward their climatological values from the FREE run. The relaxation rate for this nudging varies linearly from $0\,\mathrm{day}^{-1}$ at 64 hPa to $4\,\mathrm{day}^{-1}$ at 28 hPa, above which it is constant. This nudging has the effect of removing the zonally symmetric component of the stratospheric variability; the effects of this nudging on the tropospheric state have been discussed extensively by Simpson et al. (2011, 2013a,b), and Hitchcock and Haynes (2014). Finally, an ensemble of 5-month integrations, spun off from CTRL each 21 December, are nudged toward the time-evolving, zonally symmetric component of a reference stratospheric sudden warming produced by FREE with the same nudging configuration used in CTRL. The ensemble considered here, referred to as SSWd, is nudged toward a reference event classified (following Charlton and Polvani 2007) as a vortex displacement. While a second such ensemble, nudged toward a reference event classified as a split, was also carried out and analyzed by HS, some of the fields from the latter relevant to the present analysis are not available. The two ensembles were shown by HS to produce a very similar tropospheric response, so we focus on the first. There are two primary advantages to considering this nudged ensemble. First, any tropospheric signal seen in the SSWd ensemble must, by experimental design, ultimately be of stratospheric origin. Second, since the stratospheric anomalies are large, persistent, and nearly identical in every member, the tropospheric signal is made clearer. Nonetheless, it is useful to compare the nudged ensemble with anomalies in FREE composited during the internally generated events to verify that the response is not somehow an artifact of the nudging procedure. Six-hourly instantaneous data, interpolated onto pressure levels, are used for the calculation of all relevant budget terms.

### b. ERA-Interim

Data from ERA-Interim are also used (Dee et al. 2011). Six-hourly, model-level data spanning 1979–2014,

interpolated horizontally onto a 1° × 1° grid were used for computing the relevant budget terms, with the exception of the mountain torque term, which was computed from the surface pressure and surface orography field on the native T255 Gaussian grid used by the model. This was found to be essential for accurate results.

### c. Event definition

Stratospheric sudden warmings are identified following the criteria of Charlton and Polvani (2007). Since we are interested in understanding the shift of the zonal-mean jet, shown by HS to be produced by the stratospheric zonal-mean anomalies, we include in the composite analysis of the FREE integration only those sudden warmings that exhibit persistent anomalies in the lower stratosphere following the initial zonal-mean zonal wind reversal. We follow the identification criteria of Hitchcock et al. (2013a), who also showed that the tropospheric response to sudden warmings on time scales of 1–2 months is dominated by these large-amplitude, persistent, polar night jet oscillation events. This includes 38 of the 67 sudden warmings that are simulated by FREE; composites of this subset are found to provide a clearer and larger-amplitude signal than composites where all events are included. The events included are exactly those considered by Hitchcock and Shepherd (2013), who described aspects of their stratospheric dynamics in the same integration (FREE). The central dates, corresponding to lag 0 in figures shown below, are those of the wind reversals identified by the Charlton and Polvani (2007) criteria.

Polar night jet oscillation events in ERA-Interim are similarly identified. The central dates of the 15 events so identified are listed in Table 1.

TABLE 1. Central dates of major stratospheric sudden warmings also classified as polar night jet oscillation events used for the ERA-Interim composites.

| | | |
|---|---|---|
| 24 Feb 1984 | 21 Feb 1989 | 5 Jan 2004 |
| 1 Jan 1985 | 15 Dec 1998 | 21 Jan 2006 |
| 23 Jan 1987 | 26 Feb 1999 | 24 Jan 2009 |
| 8 Dec 1987 | 11 Feb 2001 | 9 Feb 2010 |
| 14 Mar 1988 | 30 Dec 2001 | 6 Jan 2013 |

## 3. Vertically integrated angular momentum budget

Since the tropospheric response to stratospheric sudden warmings is relatively independent of height (e.g., HS), we follow LH01/03 and focus on the wind response, vertically integrated through the troposphere. This leads to a significant simplification of the associated angular momentum budget and makes possible a very simple set of parameterizations for the eddy feedbacks. We focus first on the vertically integrated wind response itself, and then turn to the budget.

### a. Vertically integrated response

The zonal-mean zonal wind response, vertically integrated through the troposphere and cosine weighted to emphasize changes in relative angular momentum, is shown in Fig. 1 for the SSWd ensemble and the FREE composite. A 15-day low-pass Lanczos filter with 51 weights (Duchon 1979) has been applied to both cases. The vertical integral is defined as

$$[x] = \frac{1}{p_{s0} - p_t} \int_{p_t}^{p_b} x \, dp . \tag{1}$$

The upper boundary of the integral $p_t$ is set to 100 hPa, and $p_{s0}$ is 1000 hPa. The sensitivity of the results to the choice of $p_t$ will be discussed further below. In this section, the lower control surface $p_b$ is taken to be the zonal-mean surface pressure $\overline{p_s}(t, \phi)$ and, where necessary, fields on isobars that lie below the surface are extrapolated by using the value at the lowest model level. The normalization $p_t - p_{s0}$ is taken to be a constant so that (1) is proportional to the net momentum within the troposphere, as opposed to an average per unit mass within the partial column.

To give a sense for the sampling uncertainty associated with this signal, the climatological wintertime standard deviation $S_u$ of the vertically averaged relative angular momentum in Northern Hemisphere midlatitudes is roughly 2.3 m s$^{-1}$ in FREE and CTRL. Although the time-averaged position of the zonal-mean tropospheric jet shifts following sudden warmings, to leading order its standard deviation does not change (HS). Assuming each year and each event is independent, the standard deviation of the ensemble or composite mean is well estimated by

$$S_u \sqrt{N_S^{-1} + N_Y^{-1}}, \tag{2}$$

where $N_S$ is the number of sudden warmings (the number in parentheses in the panel titles of Fig. 1), and $N_Y$ is the number of years in the reference climatology. This predicts a two-sigma uncertainty of 0.7 m s$^{-1}$ for the SSWd ensemble and 0.9 m s$^{-1}$ for the FREE composite. There is some meridional dependence of these values, but they agree well with more involved calculations, including bootstrap estimates for the midlatitude wind response (not shown). While the midlatitude response shown in Fig. 1 for SSWd is roughly twice the value of the 2$\sigma$ uncertainty and is therefore well resolved, the response in FREE is roughly equal to the 2$\sigma$

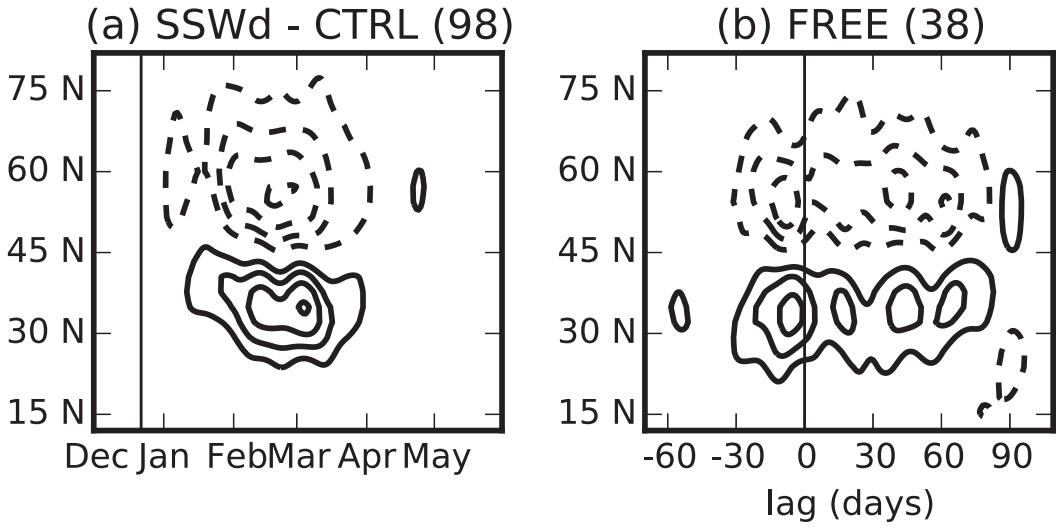


FIG. 1. Vertically integrated zonal-mean zonal wind anomalies, multiplied by the cosine of latitude in (a) the SSWd ensemble and (b) the FREE composite. Contour intervals are 0.5 m $s^{-1}$, and the zero contour is omitted. The number in parentheses in the title of each panel indicates the number of members in each ensemble/composite. The thin vertical lines indicate the date of the 10-hPa, 60°N zonal wind reversal. A low-pass 15-day Lanczos filter with 51 weights has been applied in each case.

uncertainty and is thus only marginally resolved in a pointwise sense.

In both cases the integrated response is dominated by a dipolar anomaly in the winds, with an increase to the south and a decrease to the north. The larger-amplitude response in the SSWd composite is consistent with the reference event being one of the larger-amplitude events generated by the free-running model, while the FREE composite includes events of varying magnitudes. As described in HS, although the wind reversal at 10 hPa occurs in late December in the SSWd reference event, the lower stratosphere is only perturbed by a subsequent pulse of wave activity in late January. It is only after this second episode of strong wave driving that the tropospheric anomalies arise in the SSWd ensemble. This delay between the wind reversal at 10 hPa and the onset of significant lower-stratospheric anomalies is not typical of the stratospheric warming events in FREE, and in this regard the months of February and March in the SSWd ensemble are more comparable to lags 0–60 in the FREE composite, as was discussed by HS. The FREE composite exhibits a significant shift in the jet prior to the stratospheric wind reversal, which precedes the onset of the nudging in the SSWd ensemble. Comprehensive stratosphere-resolving models disagree on the presence of this precursor [e.g., Gerber et al. (2010); see their Fig. 10]. The high-latitude response in SSWd (poleward of 65°N) is not apparent as a feature of the FREE composite, which may indicate it is a feature particular to the structure of the anomalies in the SSWd reference event. These differences notwithstanding, our focus will be on the midlatitude dipolar anomaly following the stratospheric event, which, in the SSWd ensemble, can be unambiguously attributed to the imposed zonally symmetric stratospheric anomalies by experimental design (HS).

This dipolar response projects strongly onto the first empirical orthogonal function (EOF) of the vertically integrated, deseasonalized, zonal-mean wind in boreal winter (Fig. 2). We refer to this mode as the zonal index, though it is very highly correlated with other indices of the tropospheric northern annular mode. The EOF is computed from the vertically integrated zonal-mean zonal wind from 10° to 80°N in winter (December–February). Relative to that of FREE, the structure of the first EOF in CTRL is shifted equatorward and is somewhat weaker in amplitude, as might be expected from removing the variability associated with the tropospheric response to zonal-mean stratospheric variability. The difference between CTRL and FREE arises primarily from the upper-tropospheric flow, as can be inferred from the layerwise northern annular mode (NAM) structures shown in Simpson et al. (2011).

### b. *Angular momentum budget*

The dynamics of the essentially barotropic zonal index are simplified by the near cancellation of the Coriolis torques. Departures from climatology are primarily maintained against surface friction by a shift in the angular momentum fluxes associated with eddies. We

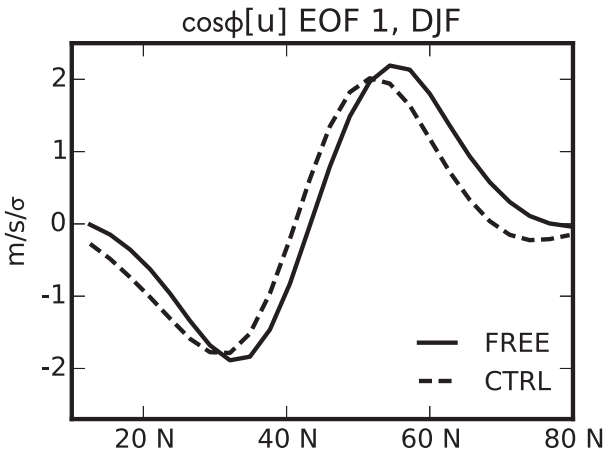


FIG. 2. First empirical orthogonal function of vertically integrated zonal-mean zonal winds from FREE and CTRL, multiplied by the cosine of latitude, computed from daily DJF variability.

therefore consider the vertically integrated zonal-mean angular momentum budget, which follows, for example, from the Eulerian mean equations given by Andrews et al. (1987). With the choice of the zonal-mean surface pressure $\overline{p_s}$ as the lower control surface $p_b$, the zonal momentum budget can be written as

$$\partial_t U = M_s + M_p + X + C + W + \varepsilon, \tag{3}$$

in which

$$\partial_t U = [\partial_t \overline{u}], \quad C = \left[\left\{f - \frac{\partial_\phi(\cos\phi\overline{u})}{a\cos\phi}\right\}\overline{v} - \overline{\omega}\partial_p\overline{u}\right]$$

$$M_s = \left[-\frac{\partial_\phi(\cos^2\phi\overline{v'u'}_{k>3})}{a\cos^2\phi}\right], \quad W = [-\partial_p(\overline{\omega'u'})]$$

$$M_p = \left[-\frac{\partial_\phi(\cos^2\phi\overline{v'u'}_{k\le3})}{a\cos^2\phi}\right], \quad X = [\overline{X}].$$

Here, overlines indicate zonal means, and primes indicate deviations from the zonal mean. The meridional momentum flux convergence has been decomposed into that due to the planetary-scale (zonal wavenumbers 1–3; $M_p$) and synoptic-scale (the remainder; $M_s$) eddies. For brevity, $M_s$ and $M_p$ will be referred to as the synoptic- and planetary-scale eddy flux terms; unless otherwise specified, this should be understood to denote their convergence. The circulation term $C$ includes all contributions that can be attributed to the mean meridional circulation, though it is dominated by the Coriolis term in the present analysis. All tendencies from parameterized processes are included in $X$, but it is dominated by surface stresses. The term $W$ is the transfer of momentum between the troposphere and stratosphere by vertical eddy-momentum fluxes. All terms are computed explicitly, except for the residual $\varepsilon$ on the right-hand side of (3), which arises primarily as a result of numerical and sampling issues and of the choice of the lower control surface.

We have chosen $p_t$ to be 100 hPa in order to include the majority of the effects of the tropospheric eddy fluxes (and the meridional circulation that they induce), while excluding as much of the stratosphere as possible. The vertical structures of these anomalous fluxes were shown in HS (their Figs. 9 and 10). The results are essentially unchanged if $p_t$ is set to 200 hPa.

The mountain torque, typically considered in zonal-mean momentum budgets, is responsible for a non-negligible exchange of angular momentum between the atmosphere and the solid earth. For a general lower control surface $p_b$, this stress takes the form

$$\frac{1}{p_{s0} - p_t}\frac{\overline{h_s\partial_\lambda p_b}}{a\cos\phi}.$$

Ideally, one would like to use the full, zonally varying surface pressure as the lower control surface, upon which the mountain torque takes its standard form:

$$M_T = \frac{1}{p_{s0} - p_t}\frac{\overline{h_s\partial_\lambda p_s}}{a\cos\phi}. \tag{4}$$

Unfortunately, data availability precludes this option. If, however, the lower control surface is independent of longitude, the mountain torque formally vanishes in the budget. It can be demonstrated with the reanalysis data that this exchange of angular momentum arises instead from the extrapolated surface stress. Including $M_T$ in this budget, therefore, would result in incorrectly double counting this stress. This is confirmed by the fact (demonstrated below) that the budget residual is larger if $M_T$ is erroneously included. Nonetheless, we show the term (4) where relevant for comparison. Note that this is also the case if $p_b$ is taken to be $p_{s0}$, as was done by LH01 and LH03. LH03 did include the mountain torque in their analysis, and this may be one reason for the unexplained budget residual they found in the Northern Hemisphere.

For our purposes, we are concerned with the relative importance of eddy forcings and zonal-mean circulation terms in driving/maintaining the tropospheric circulation anomalies. The balance we will be considering is between these forcings and the drag processes at the lower boundary. With $p_b$ set to $p_s$, these drag processes would be a combination of surface stress and mountain torque, but, in the formulation used here, they are captured by the extrapolated surface stress alone.

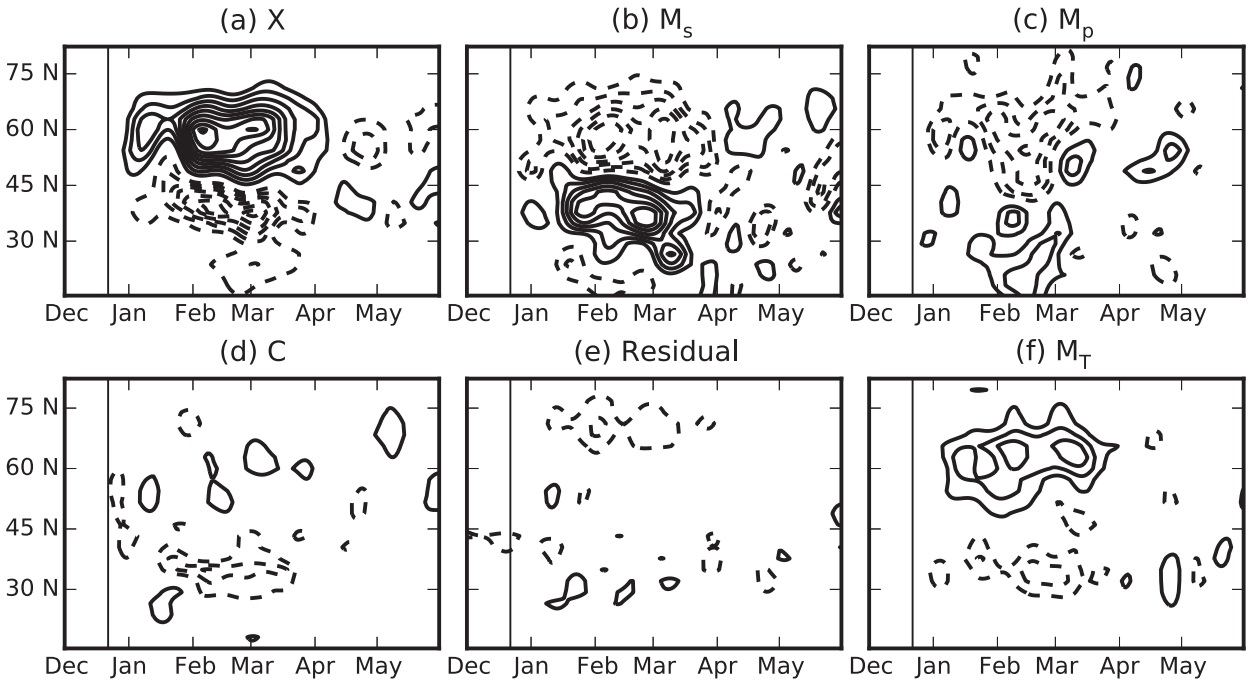


FIG. 3. Terms in the vertically integrated zonal-mean momentum budget, multiplied by cosine of latitude, from the SSWd ensemble: (a) surface stress, (b) synoptic-scale eddy flux, (c) planetary-scale eddy flux, (d) circulation, (e) budget residual (excluding the mountain torque), and (f) mountain torque. See text for definitions. In all cases, contour intervals are 0.05 m $s^{-1}$ $day^{-1}$. A 20-day low-pass Lanczos filter with 81 weights has been applied. Estimates of 95% confidence intervals (not shown) are roughly constant in time and vary in latitude from 0.05 to 0.2 m $s^{-1}$ $day^{-1}$, with smaller values at low latitudes and higher values at high latitudes for (a)–(c) and (f), and near constant values of 0.05 $s^{-1}$ $day^{-1}$ for (d).

The terms $X$, $M_s$, $M_p$, $C$, the budget residual $\varepsilon$, and $M_T$ are shown for the SSWd ensemble in Fig. 3, as anomalies from the CTRL integration. These terms are considerably noisier than the vertically integrated winds themselves, and a 20-day low-pass Lanczos filter with 81 weights has been applied so that the longer time-scale response is clarified. Closely related unfiltered time series will be shown in a later section, and discussion of the associated statistical uncertainty in these composite means is deferred until then. To a good approximation, the surface stress (Fig. 3a) is balanced throughout the composite in the ensemble average by the eddy flux terms (Figs. 3b,c). The eddy fluxes are dominated by the synoptic scales, which explain roughly two-thirds of the total anomalous convergence, with the remainder provided by the planetary-scale fluxes. The circulation term (Fig. 3d) is considerably weaker than either of the eddy flux convergence terms and is dominated in the ensemble average by a tendency to oppose the low-latitude wind changes. The vertical eddy flux term $W$ is negligible, and despite the time evolution of the zonal-mean zonal wind field evident in Fig. 1a, the acceleration term $\partial_t U$ is of the same order as the residual (not shown).

The mountain torque (Fig. 3f) is of the same order as the planetary-scale eddy flux term and broadly in the opposite sense; it is, as mentioned above, substantially larger than the residual, supporting its exclusion from the budget. This behavior is qualitatively different from the budget obtained following sudden warmings in the dry dynamical core experiments of Hitchcock et al. (2013b), where the mountain torque contribution dominated the planetary-scale momentum fluxes and contributed a substantial moderating influence on the shift of the jet. This may be a result of the much simpler specification of the topography in the dry dynamical core.

The same terms are shown for the FREE composite in Fig. 4. The overall picture in the months following the stratospheric wind reversal is quite consistent with Fig. 3, though, given the fewer events and smaller amplitude of the signal, the fields are significantly noisier. The surface stress term is reasonably well balanced by the net eddy flux terms (again dominated by synoptic-scale eddies). Consistent with the zonal wind composite (Fig. 1b), there are substantial budget anomalies several weeks prior to the midstratospheric wind reversal at lag 0. There is also a contribution from the circulation term near lag 0, which is absent in the SSWd ensemble, as expected from the arguments given in Hitchcock and Haynes (2014); note that again the contribution is in the opposite sense required to produce the tropospheric

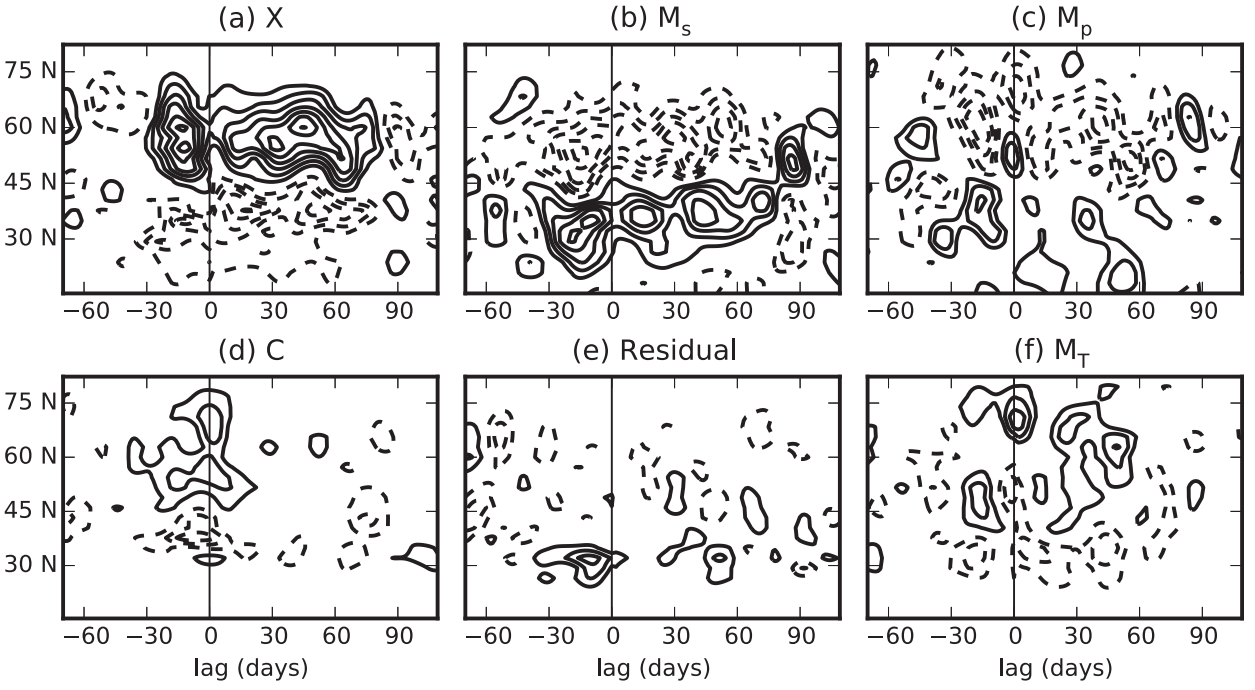


FIG. 4. As in Fig. 3, but for the FREE composite. Estimates of 95% confidence intervals show very similar structures to those for the SSWd ensemble, but with values varying from 0.1 to 0.35 m s$^{-1}$ day$^{-1}$.

wind shift. The mountain torque is of the same order as the planetary-scale flux term but, as in the SSWd ensemble, is substantially larger than the residual excluding $M_T$.

The meridional structured of most of the budget's terms are reasonably well correlated with the structure of the zonal index, though higher-frequency fluctuations are also present with other meridional structures. Since these fluctuations are weaker in the SSWd ensemble average, they are likely to be residuals of tropospheric variability unrelated to the "deterministic" component of the response to stratospheric variability. We therefore focus on the projection of these terms onto the zonal index, under the assumption that this will describe the dominant component of the zonal-mean tropospheric response.

### c. *Quantifying feedbacks*

To quantify the role of the tropospheric feedbacks, we make use of the simple parameterization of the eddy momentum fluxes following LH01/03, who also considered the meridional projection of the vertically integrated budget onto the zonal index. The simple model can be derived by projecting the budget in (3) on to the leading EOF. Using $z$ to denote the zonal index time series (i.e., the projection of the winds themselves onto the leading EOF), this can be written

$$\partial_t z = m_s + m_p + x, \tag{5}$$

in which the lowercase terms on the right-hand side indicate the projections of the corresponding uppercase terms in (3). The projected vertical eddy flux term $w$ and Coriolis term $c$ have been neglected, as has the term that arises when taking the time derivative out of the vertical average in $\partial_t U$. LH01/03 parameterized the eddy flux term $m$ (equal to $m_s + m_p$) as the sum of a stochastic process and a linear feedback term that is organized by the zonal index itself. We allow here explicitly for the planetary- and synoptic-scale terms to be distinct processes, having their own stochastic components ($\tilde{m}_s$ and $\tilde{m}_p$) and their own feedback coefficients ($b_s$ and $b_p$):

$$m_s = \tilde{m}_s + b_s z, \quad m_p = \tilde{m}_p + b_p z.$$

Also following LH01/03, the surface stress $x$ is parameterized as a simple linear relaxation of the zonal index

$$x = -kz.$$

This results in a simple, closed, stochastic model of the zonal index

$$\partial_t z = \tilde{m}_s + \tilde{m}_p - (k - b_s - b_p)z. \tag{6}$$

The lag covariance structures between the terms $z, x, m_s$, and $m_p$ predicted by this model can then be compared against those computed from the CMAM integrations.

Figure 5 shows several terms in the angular momentum budget from the CMAM integrations, projected onto the meridional structure of the Northern Hemisphere EOF then lag regressed against the principal component time series so that their amplitudes correspond to what would be expected preceding and following a shift of $1\sigma$ in the zonal index. No time filtering has been applied to the time series in this calculation. The EOF from CTRL has been used here, but the conclusions are not affected if the EOF from FREE is used instead. In addition to terms defined above, the projection of the mountain torque term $m_T$ and the budget residual are also shown.

As was shown by LH01/03 for observations, Chen and Plumb (2009) for a dry dynamical core, and Simpson et al. (2013b) for the Southern Hemisphere in FREE and CTRL, when the eddy-flux terms lead the zonal index (i.e., negative lags), their regression coefficients increase steadily with increasing lag, consistent with their role in forcing zonal-mean shifts of the jet. When the index leads the eddy flux terms by a few days, however, the regression coefficients decrease rapidly, suggesting that, on these short time scales, a significant fraction of the variability in the eddy fluxes is not organized by the state of the zonal index. When the zonal index leads the eddy flux terms by 1–2 weeks (positive lags; indicated by the vertical lines), the regression coefficients have risen again, suggesting that the state of the jet plays a role in organizing the eddies, thus providing greater predictive skill at these longer time scales. This correlation at positive lags leads LH01 and LH03 to identify a positive feedback. As discussed by LH03, this inference assumes that there is not another source of persistence organizing the eddy flux terms.

Following the methodology described in Simpson et al. (2013b), the feedback parameters $k$, $b_s$, and $b_p$ for both FREE and CTRL are fit from the regression coefficients at lags of 7–14 days, indicated by the vertical lines in Fig. 5. These are shown, with 95% confidence intervals estimated as in Simpson et al. (2013b), in (Fig. 6). This methodology controls for additional persistence in the zonal index that does not arise from internal eddy feedback processes. The three fitted parameters agree between FREE and CTRL to within statistical uncertainty. Despite the more rapid decay of the $m_p$ correlations with increasing lag in CTRL, a weak positive feedback is still inferred, although in this case the confidence intervals overlap zero.

As will be quantified below, the positive feedback parameters imply that the eddies will amplify the effects of an imposed forcing.

### d. Coupling mechanisms

To apply this model to the tropospheric response following sudden warmings, we must consider the nature

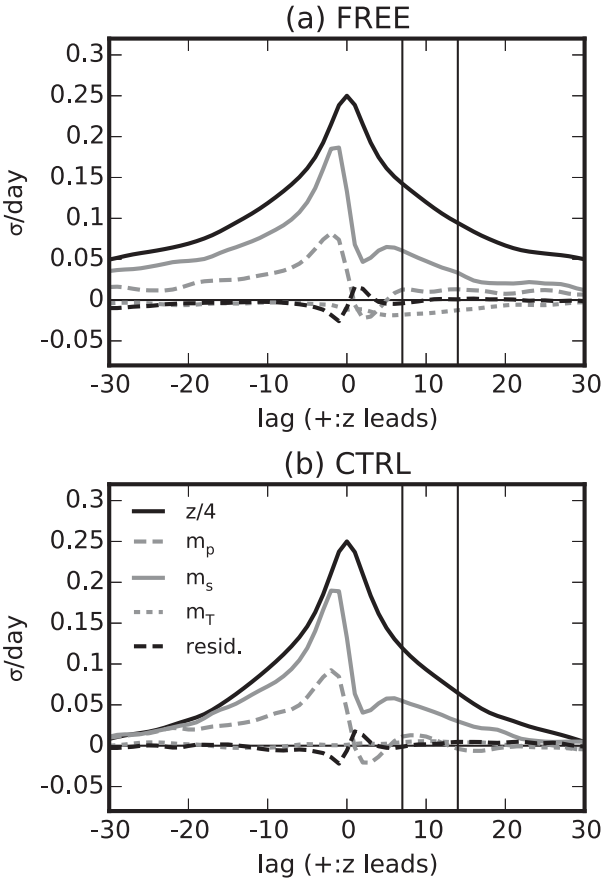


FIG. 5. Lag regressions of terms $z$, $m_s$, $m_p$, and $m_T$ and the budget residual onto the zonal index $z$ for FREE and CTRL. Positive lags indicate that the zonal index leads. The regression coefficients for $z$ are multiplied by $\frac{1}{4}$ to fit on the same vertical scale and are in units of standard deviations, unlike the remainder of the terms. The vertical lines indicate the time period used to compute the surface friction and feedback parameters (see text for details).

of the forcing on the tropospheric jet responsible for the stratospheric influence. Three possible classes of mechanisms are considered.

The first is through the zonally symmetric circulations expected as a result of downward control (Song and Robinson 2004; Thompson et al. 2006). This forcing would be imparted on the tropospheric winds through the term $c$, neglected on the rhs of (5), predominantly through the Coriolis torque itself, though meridional and vertical advection of relative angular momentum may potentially contribute as well. We interpret contributions from these terms in the ensemble-mean anomalies as an effective forcing from the stratosphere, renaming them $F_c$:

$$\partial_t z = m_s + m_p + F_c - kz\,. \tag{7}$$

Note that, as argued by Hitchcock and Haynes (2014), the nudging is expected to reproduce any such contributions

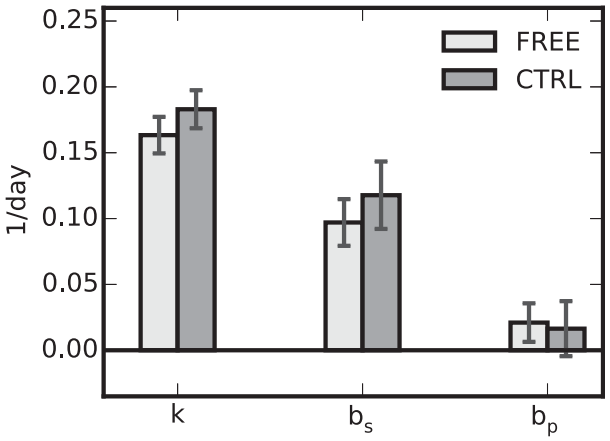


FIG. 6. Surface stress and eddy-feedback terms estimated by the regression methodology (see text) for FREE and CTRL. Error bars indicate 95% confidence intervals estimated by a bootstrap method.

from the circulation term with the exception of the brief period during the onset of the warming, as mentioned in the discussion of Fig. 4.

The second class of mechanisms includes those by which the stratosphere influences the synoptic-scale eddies directly (Wittman et al. 2007; Simpson et al. 2009), as opposed to through the shift in the zonal index itself. If we assume that the linear feedback mechanism as quantified in the previous section remains relevant to the forced response in the months following the sudden warming, the stratospheric influence must arise as a component of the synoptic-scale eddy flux term that is not explained by the feedback yet still persists in the ensemble and composite averages. This assumption is justified on several grounds. Since the magnitude of the zonal index anomaly shown in Fig. 1 is roughly $0.5\sigma$, the typical jet configuration following sudden warmings is well sampled by the internal variability of the troposphere, and therefore the lag regressions should still characterize the behavior of the eddies. This is supported by the fact that the autocorrelation function of the 500-hPa NAM in the SSWd ensemble is unchanged from that obtained in CTRL (HS; see their Fig. 6b). Moreover, the synoptic-scale feedback parameter in FREE is not significantly altered in CTRL when stratospheric variability has been suppressed (Fig. 6), suggesting that the presence of sudden warmings is a weak perturbation to the statistical character of the tropospheric variability. We therefore define

$$m_s = \tilde{m}_s + b_s z + F_s, \tag{8}$$

interpreting the residual momentum flux $F_s$ that is unexplained by the parameterized feedback as being forced by the stratospheric anomalies.

Finally, the third class of mechanisms we consider is those in which the stratosphere influences the planetary-scale momentum fluxes directly (Song and Robinson 2004). As in the synoptic-scale case just described, these would arise in the zonal index budget through a component of $m_p$ (termed $F_p$) that persists in the ensemble and composite average but is not explained by the linear feedback:

$$m_p = \tilde{m}_p + b_p z + F_p. \tag{9}$$

Similar arguments to those given for the synoptic-scale feedback imply that the estimated planetary-scale feedback $b_p$ is likely to be appropriate.

In the ensemble mean, the stochastic components vanish, and thus the steady-state response to the net forcing ($F = F_c + F_s + F_p$) is given by

$$z = \frac{F}{k - b_s - b_p} = \frac{k}{k - b_s - b_p}\frac{F}{k}.$$

The tropospheric feedbacks can thus been seen to provide an amplification of the response by a factor of $k/(k - b_s - b_p)$.

## 4. Results

We are now in a position to apply the simple model to the tropospheric response in the SSWd ensemble and FREE composite. Feedback parameters fit to CTRL will be used in the following analysis; however, using the corresponding parameters from FREE does not affect any conclusions.

The surface stress $x$ in the SSWd ensemble average and in the composite average of FREE is shown in Figs. 7a and 7b and compared with the prediction of the simple linear parameterization $-kz$, in which the value fit to the CTRL run variability is used for $k$ and the time series of the zonal index from the corresponding ensemble or composite mean is used for $z$. In both cases the raw, unfiltered time series of the surface stress term computed from the full model and that computed with the linear parameterization are shown in solid lines, while the shading shows an estimate of the corresponding 95% confidence intervals. These are estimated by taking into account uncertainty in both the zonal index response and in the coefficient $k$ and are shown as an envelope centered about a smoothed version of the time series. The same 20-day, 81-weight Lanczos filter used in Figs. 3 and 4 is used for this smoothing. In both cases, the parameterized linear friction provides a good estimate of the net response of the surface stress.

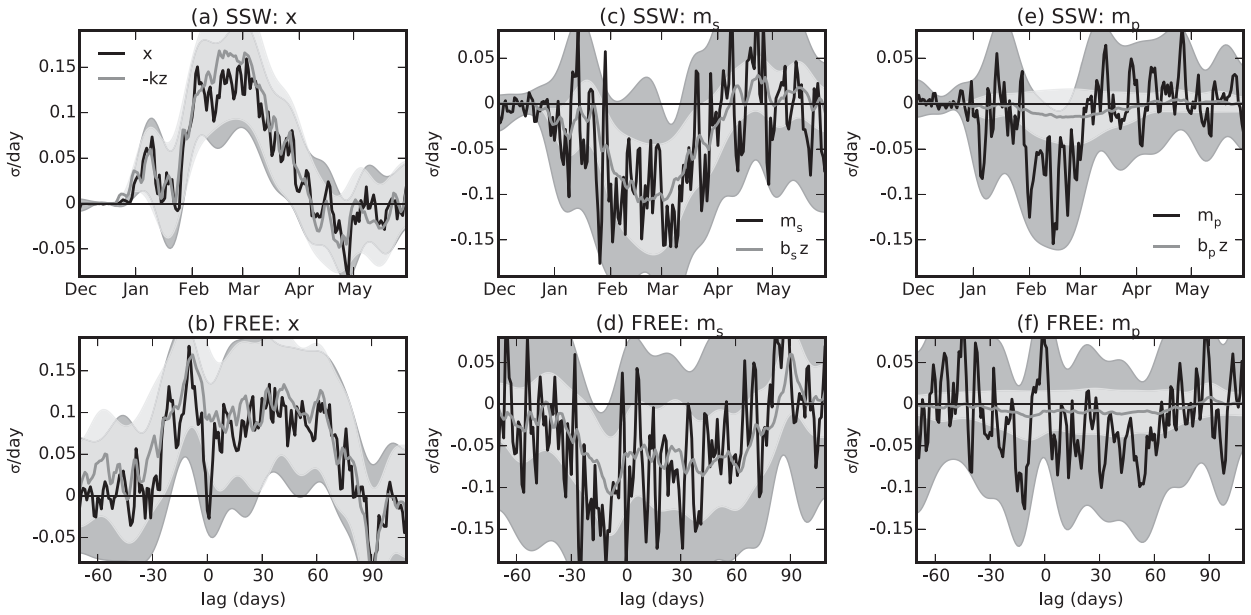


FIG. 7. Time series of the projected budget terms in (a),(c),(e) the SSWd ensemble and (d),(e),(f) the FREE composite for (a),(b) the surface stress; (c),(d) the synoptic-scale eddy fluxes; and (e),(f) the planetary-scale eddy fluxes. In all cases, the dark lines are time series computed directly from the comprehensive model, while the lighter lines are the time series predicted by the simple model parameterizations, given the full model zonal index anomalies. The shading indicates 95% confidence intervals in each case.

The explicit synoptic-scale eddy flux time series $m_s$ and parameterized feedback $b_s z$ are shown in Figs. 7c and 7d. The synoptic-scale fluxes are very well predicted by the parameterized feedback in both the SSWd ensemble and the FREE composite despite the considerable noise present in both time series. The close agreement over the several months of anomalous conditions implies that the stratosphere is not imposing a significant influence on the synoptic-scale eddies beyond the feedback induced through the zonal index anomalies, but rather that the synoptic-scale response can be explained by the tropospheric feedback alone. This is consistent with the findings of Garfinkel and Waugh (2014), who showed that the response of Rossby wave breaking was strongly correlated with the shift of the tropospheric jet, independent of the means by which this shift is induced.

Similar plots of the planetary-scale eddy flux $m_p$ and parameterized feedback $b_p z$ are shown in Figs. 7e and 7f. In contrast with the synoptic-scale fluxes, the planetary-scale fluxes are not predicted by the parameterized feedback. This is again true of both the SSWd ensemble and the FREE composite, although the signal is better resolved in the SSWd ensemble. This implies that the stratospheric anomalies influence the tropospheric planetary-scale eddies more directly, and they then act as a forcing on the zonal index, as was argued more qualitatively by HS.

The results are summarized in Figs. 8a and 8b, which show the same quantities, now time averaged over the duration of the stratospheric event: February and March for the SSWd ensemble and lags 0–60 for the FREE ensemble. The terms explicitly evaluated from the comprehensive model are shown in the dark gray bars, while the corresponding terms predicted by the simple parameterizations are shown in lighter gray. The amplitudes of the forcing terms $F_s$ and $F_p$ are estimated from (8) and (9), respectively, assuming that $\tilde{m}_s$ and $\tilde{m}_p$ vanish in the ensemble/composite mean, while $F_c$ is simply taken equal to $c$. In both the ensemble mean and the composite, $F_p$ dominates the forcing, while $F_s$ is negligible, and $F_c$ is weakly negative. Decomposing the already noisy momentum fluxes in this way is statistically demanding, and, despite the relatively large number of events in the SSWd ensemble, the uncertainties are of the same order as the forcing terms themselves. Moreover, the response of the zonal index, the surface stress, and the synoptic-scale eddy flux term are consistent with the steady-state predictions of the simple model if one imposes the value of $F_p$ estimated above (not shown), although this is essentially true by construction so long as the time tendency $z_t$ is small and the surface stress is well estimated by $-kz$.

These results suggest that the most important coupling mechanism in the CMAM integrations is in fact the organization of the tropospheric planetary-scale waves

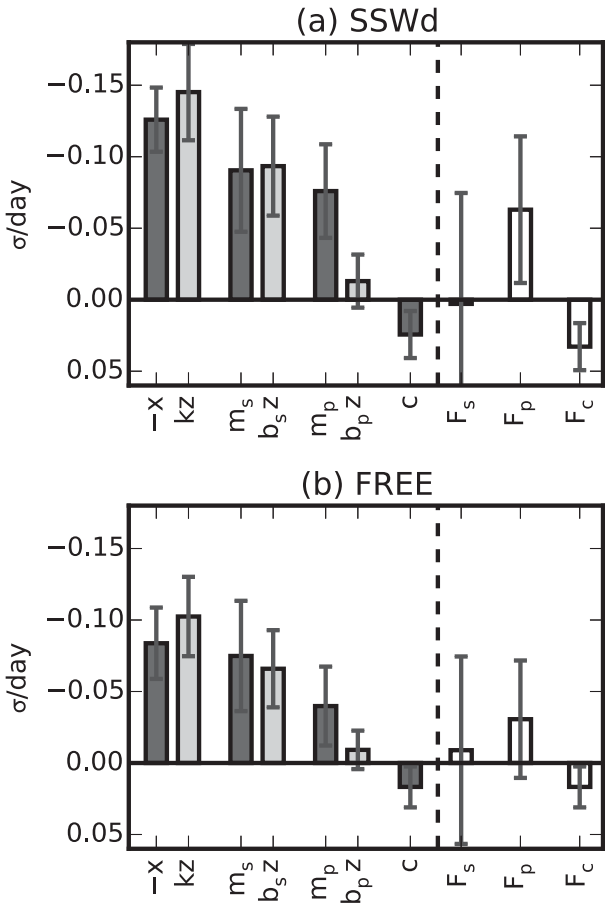


FIG. 8. Time-averaged, projected budget terms, parameterized quantities, and estimated forcing terms for (a) the SSWd ensemble and (b) the FREE composite.

by the anomalous stratospheric state. This is in line with Song and Robinson (2004) and Smith and Scott (2016) and indicates that the influence of the zonally symmetric circulation (Thompson et al. 2006) and of mechanisms by which the stratosphere might influence the tropospheric synoptic-scale eddies directly (Wittman et al. 2007; Simpson et al. 2009) are relatively unimportant to the tropospheric response to sudden warmings in CMAM.

## 5. Discussion and conclusions

The vertically integrated zonal-mean, angular momentum budget following stratospheric sudden warmings has been analyzed in a set of integrations of the Canadian Middle Atmosphere Model. Consistent with other studies, it is found that the dominant response following a stratospheric event is an equatorward shift of the midlatitude jet. The shift projects strongly onto the first EOF of the DJF variability in the free-running version of the model. The projected response is further analyzed in the context of the simple feedback model of LH01 and LH03. In particular, the eddy fluxes of momentum associated with synoptic- and planetary-scale eddies are each parameterized as a combination of a stochastic component and a linear feedback term, proportional to the principal component time series of the EOF itself. The parameters for this feedback, as well as for the linear parameterization of the surface stress, are fit to the internal variability of the model (Figs. 5, 6).

When applied to the forced response problem, it is found that the surface stress anomalies produced by the comprehensive model are well predicted by the simple linear parameterization (Figs. 7a,d). Moreover, the response of the synoptic-scale eddy fluxes is also well predicted by the parameterized feedback, suggesting that this response can be explained entirely by this feedback, and not by any direct organization of the synoptic-scale eddies by the stratospheric flow itself (Figs. 7b,e). In contrast, while the anomalous planetary-scale momentum fluxes provide a smaller net contribution to the shift, they are not explained by the parameterized feedback (Figs. 7c,f) but rather appear to be organized by the stratospheric anomalies themselves and thus provide the relevant forcing. The projection of the anomalous Coriolis force (and other zonally symmetric advection terms) onto the zonal index is weak (Fig. 8), indicating that the effects of the downward control response to the stratospheric anomalies are negligible and, if anything, negative.

Thus the analysis indicates the key mechanism for the downward coupling, at least in CMAM, involves the tropospheric planetary waves, which are modified by the stratospheric anomalies, and further study of this influence is warranted. Improvements in our understanding of the tropospheric response to stratospheric sudden warmings and to more general classes of forcings are likely to follow. It seems therefore appropriate to speculate briefly on possible mechanisms by which this influence might be imparted. Assuming there is no significant source of waves within the stratosphere, several possibilities exist. One is that the state of the stratosphere is relevant for the amplitude of the waves throughout the depth of the atmosphere, as is the case for the barotropic mode discussed by Esler and Scott (2005) and Matthewman and Esler (2011). A second possibility is that a significant reflected component of the waves is always present, and it is this component that is being modulated by the anomalous stratospheric state. Another possibility is that lower-stratospheric anomalies have an effect on the propagation of tropospheric planetary waves. Finally, it is also conceivably possible that the planetary wave anomalies

are themselves produced indirectly, in response to a stratospheric influence on some tropospheric-flow structure that does not project onto the zonal index. Determining whether any of these mechanisms are relevant is beyond the scope of this work but is an essential question for further study.

While the approach followed here is close in spirit to the use of the fluctuation–dissipation theorem (FDT) to predict a forced response, it differs in its quantitative predictions. As a result of the serial correlations present in the stochastic terms $\tilde{m}_s$ and $\tilde{m}_p$ (pointed out by LH03), the autocorrelation of $z$ will differ from the simple exponential form $\rho(t) = \exp[-(k - b_s - b_p)t]$, which holds only if these terms are serially uncorrelated white noise. As a result, the FDT, applied directly to the simple model of LH01/03, overpredicts the response to a steady-state forcing. This is because of the presence of nonnegligible time scales present in the dynamics of the zonally asymmetric eddies. This issue is distinct from the presence of external forcings with long time scales, identified in the Southern Hemisphere by Simpson et al. (2013b), and amounts to a further reason to be cautious in connecting estimates of the decorrelation time scale with the strength of relevant feedback processes. One perspective to take on this failure is that, by focusing only on the zonal index itself, the system has been too highly truncated, and that some of the essential details of the lag correlation structures required for the FDT to correctly predict the forced response are being lost by this truncation. An essential question to address for efforts to apply the FDT, then, is that of which degrees of freedom to include. We note that time scales relevant to this particular failure are likely to be found in the zonally asymmetric components, which have been neglected in some previous attempts to apply the FDT (e.g., Ring and Plumb 2008).

The success of the Lorenz and Hartmann model in describing the tropospheric response to stratospheric sudden warmings provides a quantitative justification for the ''ringing bell'' analogy often invoked to understand the similarity of the tropospheric response to many different types of external forcings, since the feedback has a preferred meridional structure. This analogy should not be taken too far, however, as the feedback is not (in this framework) the result of the resonance of a free mode of the system. On the longer time scales relevant for sudden warmings, the shift must be maintained by stratospheric conditions, since in their absence the statistics of the tropospheric flow should return rapidly to their undisturbed state. A corollary of this is that the persistence of the stratospheric perturbation is essential, and thus differences in, for instance, splits and displacements that persist for only a week or so after the onset of the event are unlikely to be relevant to the response on longer time scales (Maycock and Hitchcock 2015).

This analysis also suggests a general approach to separating internal feedbacks from the direct influence imparted by a given forcing: if the feedback can be quantified, its contribution can be diagnostically removed from the response, revealing the relevant forcing. However, this requires an accurate quantification of the processes responsible for the feedback and presents the difficulty (in the case of a positive feedback) that the residual will be even more difficult to resolve statistically than the full response. These requirements may remain too demanding in the context of observational studies without a more effective means of controlling for the internal variability. However, given the ever-increasing computational power available, the use of appropriate numerical experiments would seem a promising approach for yielding deeper insight into the dynamical responses produced by comprehensive models.

*Acknowledgments.* PH acknowledges funding support from the European Research Council through the ACCI project (Grant 267760) lead by John Pyle and from an NSERC postdoctoral fellowship. IRS acknowledges support from National Science Foundation funding to the National Center for Atmospheric Research and NSF Award AGS-1317469.

## APPENDIX

### Reanalysis Results

A natural question is whether a similar analysis can be applied to the reanalysis data. Unfortunately, as discussed in the introduction, a number of issues arise. We present these details here.

The composite of the vertically integrated zonal-mean wind anomalies is shown for three choices of $p_b$: the constant value $p_{s0}$ (Fig. A1a), the zonal mean surface pressure $\overline{p_s}(t, \phi)$ (Fig. A1b), and the zonally varying surface pressure $p_s(t, \phi, \lambda)$ (Fig. A1c). In all cases, the composite shows a midlatitude anomaly that persists for roughly 2 months following the stratospheric wind reversal, similar to that seen in the CMAM response. The reanalysis also shows a subtropical wind anomaly not apparent in the CMAM composite or ensemble, particularly from days 30 to 60 following the stratospheric wind reversal. Following LH03, we considered regressing the zonal index anomalies against an ENSO index, and at least part of this can be attributed to the, on average, weakly negative phase of ENSO during these events. However, the high-latitude weakening of the

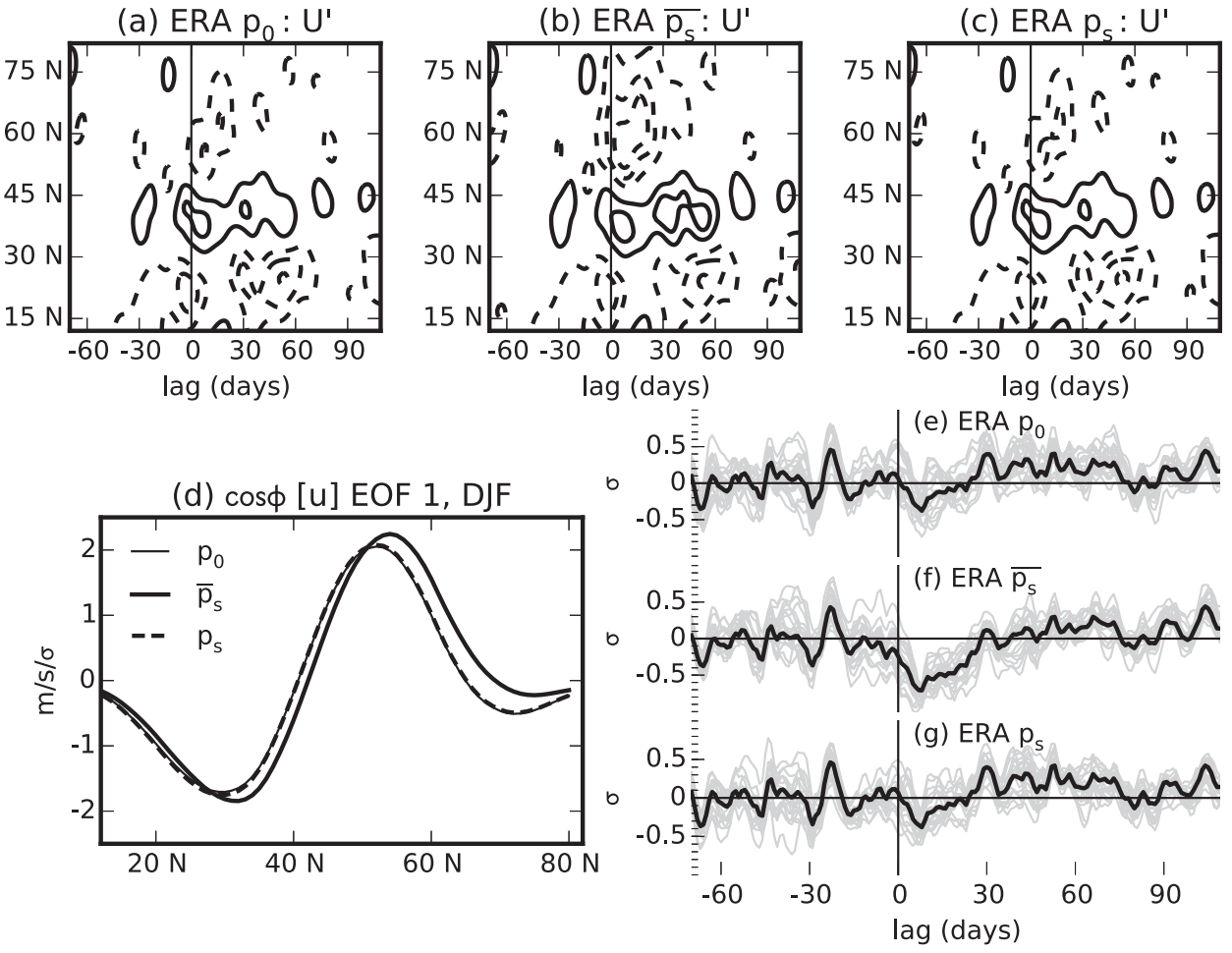


FIG. A1. (a)–(c) Composite of vertically integrated zonal-mean zonal wind anomalies in ERA-Interim, using events in Table 1. Three different lower control surfaces are used: (a) $p_{s0}$, (b) $\overline{p_s}$, and (c) $p_s$; see text for details. (d) Leading EOF of vertically integrated zonal-mean zonal winds using the three different control surfaces, weighted by the cosine of latitude. (e)–(g) Time series of the projection of the composite anomalies in (a)–(c) onto the corresponding leading EOF shown in (d) for the three choices of lower control surfaces.

winds following the warmings is very sensitive to the choice of the lower control surface: it is present if the zonal-mean surface pressure is used, but not in the other two cases, suggesting that there is a significant high-latitude response on isobars that lie within the atmosphere but below the zonal-mean surface pressure. This sensitivity is not found in either the SSWd ensemble or the FREE composite. The pointwise $2\sigma$ uncertainty in the midlatitudes given by (2) is $1.4\,\mathrm{m\,s^{-1}}$, about twice that of the SSWd ensemble, and significantly larger than the anomalies seen, suggesting these patterns are still strongly affected by statistical noise.

The leading EOFs of the vertically integrated zonal-mean zonal wind for the three choices of $p_b$ are shown in Fig. A1d. Following LH03, the effects of ENSO are taken into account by first removing variability that is linearly correlated with the Niño-3.4 index as computed from the sea surface temperatures used by ERA-Interim. This is also done for the lag regressions below, though the effects in both cases are minor and do not affect any conclusions. In all cases, the leading EOF exhibits the expected dipolar structure. However, while the EOF for the choice of constant $p_{s0}$ and the full, zonally varying surface pressure are very similar, the use of the zonally symmetric surface pressure results in an EOF with a node at somewhat higher latitude.

The projections of the composite anomalies onto these meridional structures in the three cases are shown in Figs. A1e–g, with bootstrap estimates of the associated uncertainty. Note these only take into account uncertainty associated with the interevent variability, not the uncertainty in the observed climatology [which can be expected from (2) to add an additional 20% to the uncertainty], or in the structure of the EOF. In strong

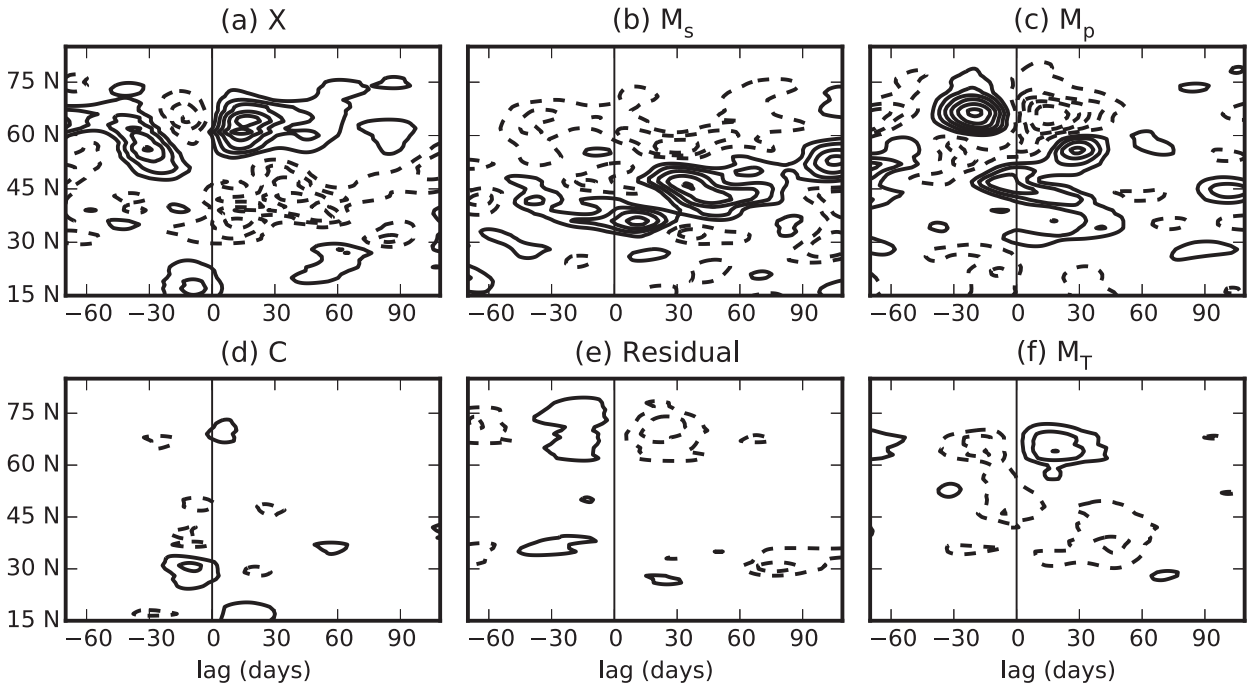


FIG. A2. As in Fig. 3, but for the ERA-Interim composite with $p_b = \overline{p_s}$. A 40-day low-pass Lanczos filter with 121 weights has been applied.

contrast to the results from CMAM, where the anomaly projected dominantly onto the leading EOF, and despite the presence of significant midlatitude anomalies in Figs. A1a–c, the projection of the anomalies is negative only for the first 20–30 days, and the magnitude of the projection is substantially weaker if $p_{s0}$ or $p_s$ is used as the lower control surface instead of $\overline{p_s}$. This appears to be a result of using zonally symmetric EOFs, as the composites of Baldwin and Dunkerton (2001) show significant signal for the duration of the stratospheric anomalies in contrast to those shown in HS (their Fig. 1), which more closely resemble the results in Fig. A1.

The composites of terms in the vertically integrated zonal momentum budget are shown in Fig. A2, similar to Figs. 3 and 4, with $p_b$ chosen to be $\overline{p_s}$. Focusing on the 2 months following the stratospheric wind reversal at lag 0, the broad details of the budget are consistent with that obtained in CMAM. The surface stress is again balanced by the sum of the eddy flux terms, with a negligible contribution from the circulation term. There are significant contributions from both synoptic-scale and planetary-scale eddies, although the latter appear to be stronger at higher latitudes than in CMAM. Note, however, the statistical uncertainty is roughly twice that of the SSWd budget terms, consistent with the shorter record (the climatological standard deviations of the relevant terms are quite comparable with those in CMAM). Once again, the mountain torque tends to oppose the shift of the jet; it is still the case that including it in the budget increases the size of the residual (not shown). The circulation term is negligible. Other choices of lower control surface look similar, with the exception that the surface stress is weaker when no extrapolation is carried out.

While these structures cannot be explained using only the zonal index, it is nonetheless informative to present the feedback analysis for the reanalysis as an update to LH03. This is shown in Fig. A3a for the case $p_b = \overline{p_s}$. The corresponding feedback parameters are shown in Fig. A3b for all three choices; this can be compared with the parameters fit to CMAM in Fig. 6. The surface stress parameter $k$ for the zonally symmetric lower control surfaces is in good agreement with CMAM values, but the value for the choice $p_b = p_s$ is somewhat lower; this is a result of extrapolating below the surface, and the corresponding stress is picked up predominantly by the mountain torque. The synoptic-scale feedback parameter $b_s$, however, is robust to the choice of lower control surface and is substantially weaker than those fit to the FREE and CTRL integrations of CMAM (although the uncertainty intervals do overlap with that of $b_s$ in FREE). The planetary-scale feedback parameter $b_p$ is somewhat less robust to the choice of lower control surface, though the parameters agree for all choices of $p_b$ as well as with the CMAM parameters to within the statistical uncertainty. Note that differences between this figure and those shown in LH03 (see both their Figs. 6 and 8) are demonstrably a result of the different

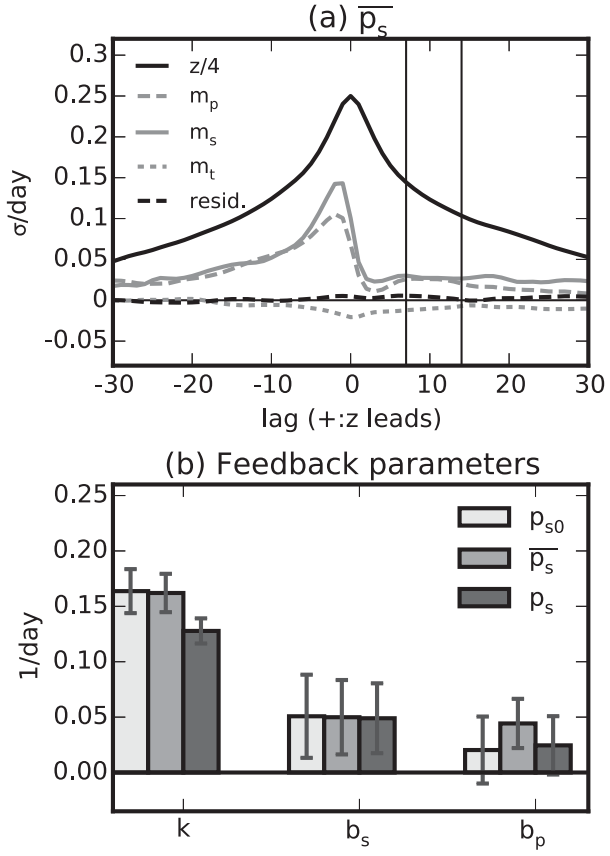


FIG. A3. (a) Lag regressions of various terms in the vertically integrated momentum budget (similar to Fig. 5) of ERA-Interim for the lower control surface $\overline{p_s}$. (b) Surface stress and eddy-feedback parameters estimated from the lag regressions for the three choices of lower control surface (similar to Fig. 6).

means of filtering the eddies; we have used here a filter based on zonal wavenumber rather than frequency.

The relatively weak projection of the composite response onto the zonal index and the small signal-to-noise ratio preclude any attempt to isolate the stratospheric influence using the methods described in the previous section, at least without significant modifications beyond the scope of this paper. It is plausibly consistent with the estimated uncertainties that this weak projection is a result of the small sample size and that the structure of the zonal-mean response would be more dominated by the leading EOF if more events were available. There are also sources of variability in the reanalysis that are not represented by the model that may affect the structure of the EOF but not the response to sudden warmings. A third possibility is that the storm tracks in the Atlantic and Pacific basins are less aligned with latitude circles and with each other than in CMAM, so the zonally averaged analysis is less able to capture the relevant feedback processes.

Nonetheless, given the close similarity found by HS of the surface response in the SSWd ensemble and the composite of events in ERA-Interim, it seems unlikely that the coupling processes in CMAM are fundamentally different from those in the real atmosphere. Indeed, there is a significant contribution from the planetary-scale momentum fluxes following the warming, as shown in Fig. A3, and while the stratospheric influence cannot be isolated in the observations, they are consistent with the conclusion from CMAM that the influence of the stratosphere is imparted through planetary-scale eddies.

## REFERENCES


Andrews, D. G., J. R. Holton, and C. B. Leovy, 1987: *Middle Atmosphere Dynamics.* International Geophysics Series, Vol. 40, Academic Press, 489 pp.

Baldwin, M. P., and T. J. Dunkerton, 2001: Stratospheric harbingers of anomalous weather regimes. *Science*, **294**, 581–584, doi:10.1126/science.1063315.

Chan, C. J., and R. A. Plumb, 2009: The response to stratospheric forcing and its dependence on the state of the troposphere. *J. Atmos. Sci.*, **66**, 2107–2115, doi:10.1175/2009JAS2937.1.

Charlton, A. J., and L. M. Polvani, 2007: A new look at stratospheric sudden warmings. Part I: Climatology and modelling benchmarks. *J. Climate*, **20**, 449–469, doi:10.1175/JCLI3996.1.

——, A. O'Neill, P. Berrisford, and W. A. Lahoz, 2005: Can the dynamical impact of the stratosphere on the troposphere be described by large-scale adjustment to the stratospheric PV distribution? *Quart. J. Roy. Meteor. Soc.*, **131**, 525–543, doi:10.1256/qj.03.222.

Chen, G., and R. A. Plumb, 2009: Quantifying the eddy feedback and the persistence of the zonal index in an idealized atmospheric model. *J. Atmos. Sci.*, **66**, 3707–3720, doi:10.1175/2009JAS3165.1.

Dee, D. P., and Coauthors, 2011: The ERA-Interim reanalysis: Configuration and performance of the data assimilation system. *Quart. J. Roy. Meteor. Soc.*, **137**, 553–597, doi:10.1002/qj.828.

DeWeaver, E., and S. Nigam, 2000: Do stationary waves drive the zonal-mean jet anomalies of the northern winter? *J. Climate*, **13**, 2160–2176, doi:10.1175/1520-0442(2000)013<2160:DSWDTZ>2.0.CO;2.

Duchon, C. E., 1979: Lanczos filtering in one and two dimensions. *J. Appl. Meteor.*, **18**, 1016–1022, doi:10.1175/1520-0450(1979)018<1016:LFIOAT>2.0.CO;2.

Esler, J. G., and R. K. Scott, 2005: Excitation of transient Rossby waves on the stratospheric polar vortex and the barotropic sudden warming. *J. Atmos. Sci.*, **62**, 3661–3682, doi:10.1175/JAS3557.1.

Garfinkel, C., and D. W. Waugh, 2014: Tropospheric Rossby wave breaking and variability of the latitude of the eddy-driven jet. *J. Climate*, **27**, 7069–7085, doi:10.1175/JCLI-D-14-00081.1.

——, ——, and E. P. Gerber, 2013: The effect of tropospheric jet latitude on coupling between the stratospheric polar vortex and the troposphere. *J. Climate*, **26**, 2077–2095, doi:10.1175/JCLI-D-12-00301.1.

Gerber, E. P., and Coauthors, 2010: Stratosphere–troposphere coupling and annular mode variability in chemistry–climate models. *J. Geophys. Res.*, **115**, D00M06, doi:10.1029/2009JD013770.

Haynes, P. H., C. J. Marks, M. E. McIntyre, T. G. Shepherd, and K. P. Shine, 1991: On the "downward control" of extratropical

diabatic circulations by eddy-induced mean zonal forces. *J. Atmos. Sci.*, **48**, 651–678, doi:10.1175/1520-0469(1991)048<0651:OTCOED>2.0.CO;2.

Hitchcock, P., and T. G. Shepherd, 2013: Zonal-mean dynamics of extended recoveries from stratospheric sudden warmings. *J. Atmos. Sci.*, **70**, 688–707, doi:10.1175/JAS-D-12-0111.1.

——, and P. H. Haynes, 2014: Zonally symmetric adjustment in the presence of artificial relaxation. *J. Atmos. Sci.*, **71**, 4349–4368, doi:10.1175/JAS-D-14-0013.1.

——, and I. R. Simpson, 2014: The downward influence of stratospheric sudden warmings. *J. Atmos. Sci.*, **71**, 3856–3876, doi:10.1175/JAS-D-14-0012.1.

——, T. G. Shepherd, and G. L. Manney, 2013a: Statistical characterization of Arctic polar-night jet oscillation events. *J. Climate*, **26**, 2096–2116, doi:10.1175/JCLI-D-12-00202.1.

——, ——, M. Taguchi, S. Yoden, and S. Noguchi, 2013b: Lower-stratospheric radiative damping and polar-night jet oscillation events. *J. Atmos. Sci.*, **70**, 1391–1408, doi:10.1175/JAS-D-12-0193.1.

Keeley, S. P. E., R. T. Sutton, and L. C. Shaffrey, 2009: Does the North Atlantic Oscillation show unusual persistence on intraseasonal timescales? *Geophys. Res. Lett.*, **36**, L22706, doi:10.1029/2009GL040367.

Kidston, J., and E. P. Gerber, 2010: Intermodel variability of the poleward shift of the austral jet stream in the CMIP3 integrations linked to biases in 20th century climatology. *Geophys. Res. Lett.*, **37**, L09708, doi:10.1029/2010GL042873.

——, A. A. Scaife, S. C. Hardiman, D. M. Mitchell, N. Butchart, M. P. Baldwin, and L. J. Gray, 2015: Stratospheric influence on tropospheric jet streams, storm tracks and surface weather. *Nat. Geosci.*, **8**, 433–440, doi:10.1038/ngeo2424.

Kushner, P. J., and L. M. Polvani, 2004: Stratosphere–troposphere coupling in a relatively simple AGCM: The role of eddies. *J. Climate*, **17**, 629–639, doi:10.1175/1520-0442(2004)017<0629:SCIARS>2.0.CO;2.

Leith, C. E., 1975: Climate response and fluctuation dissipation. *J. Atmos. Sci.*, **32**, 2022–2026, doi:10.1175/1520-0469(1975)032<2022:CRAFD>2.0.CO;2.

Limpasuvan, V., D. W. J. Thompson, and D. L. Hartmann, 2004: The life cycle of the Northern Hemisphere sudden stratospheric warmings. *J. Climate*, **17**, 2584–2596, doi:10.1175/1520-0442(2004)017<2584:TLCOTN>2.0.CO;2.

Lorenz, D. J., and D. L. Hartmann, 2001: Eddy–zonal flow feedback in the Southern Hemisphere. *J. Atmos. Sci.*, **58**, 3312–3327, doi:10.1175/1520-0469(2001)058<3312:EZFFIT>2.0.CO;2.

——, and ——, 2003: Eddy–zonal flow feedback in the Northern Hemisphere winter. *J. Climate*, **16**, 1212–1227, doi:10.1175/1520-0442(2003)16<1212:EFFITN>2.0.CO;2.

Matthewman, N. J., and J. G. Esler, 2011: Stratospheric sudden warmings as self-tuning resonances. Part I: Vortex splitting events. *J. Atmos. Sci.*, **68**, 2481–2504, doi:10.1175/JAS-D-11-07.1.

Maycock, A. C., and P. Hitchcock, 2015: Do split and displacement sudden stratospheric warmings have different annular mode signatures? *Geophys. Res. Lett.*, **42**, 10 943–10 951, doi:10.1002/2015GL066754.

Polvani, L. M., and P. J. Kushner, 2002: Tropospheric response to stratospheric perturbations in a relatively simple general circulation model. *Geophys. Res. Lett.*, **29**, 18-1–18-4, doi:10.1029/2001GL014284.

Ring, M. J., and R. A. Plumb, 2008: The response of a simplified GCM to axisymmetric forcings: Applicability of the fluctuation–dissipation theorem. *J. Atmos. Sci.*, **65**, 3880–3898, doi:10.1175/2008JAS2773.1.

Robinson, W. A., 1996: Does eddy feedback sustain variability in the zonal index. *J. Atmos. Sci.*, **53**, 3556–3569, doi:10.1175/1520-0469(1996)053<3556:DEFSVI>2.0.CO;2.

——, 2000: A baroclinic mechanism for the eddy feedback on the zonal index. *J. Atmos. Sci.*, **57**, 415–422, doi:10.1175/1520-0469(2000)057<0415:ABMFTE>2.0.CO;2.

Scinocca, J. F., N. A. McFarlane, M. Lazare, J. Li, and D. Plummer, 2008: The CCCma third generation AGCM and its extension into the middle atmosphere. *Atmos. Chem. Phys.*, **8**, 7055–7074, doi:10.5194/acp-8-7055-2008.

Sigmond, M., J. F. Scinocca, V. V. Kharin, and T. G. Shepherd, 2013: Enhanced seasonal forecast skill following stratospheric sudden warmings. *Nat. Geosci.*, **6**, 98–102, doi:10.1038/ngeo1698.

Simpson, I. R., and L. M. Polvani, 2016: Revisiting the relationship between jet position, forced response, and annular mode variability in the southern midlatitudes. *Geophys. Res. Lett.*, **43**, 2896–2903, doi:10.1002/2016GL067989.

——, M. Blackburn, and J. D. Haigh, 2009: The role of eddies in driving the tropospheric response to stratospheric heating perturbations. *J. Atmos. Sci.*, **66**, 1347–1365, doi:10.1175/2008JAS2758.1.

——, ——, ——, and S. N. Sparrow, 2010: The impact of the state of the troposphere on the response to stratospheric heating in a simplified GCM. *J. Climate*, **23**, 6166–6185, doi:10.1175/2010JCLI3792.1.

——, P. Hitchcock, T. G. Shepherd, and J. F. Scinocca, 2011: Stratospheric variability and tropospheric annular-mode timescales. *Geophys. Res. Lett.*, **38**, L20806, doi:10.1029/2011GL049304.

——, ——, ——, and ——, 2013a: Southern annular mode dynamics in observations and models. Part I: The influence of climatological zonal wind biases in a comprehensive GCM. *J. Climate*, **26**, 3953–3967, doi:10.1175/JCLI-D-12-00348.1.

——, T. G. Shepherd, P. Hitchcock, and J. F. Scinocca, 2013b: Southern annular mode dynamics in observations and models. Part II: Eddy feedbacks. *J. Climate*, **26**, 5220–5241, doi:10.1175/JCLI-D-12-00495.1.

Smith, K. L., and R. K. Scott, 2016: The role of planetary waves in the tropospheric jet response to stratospheric cooling. *Geophys. Res. Lett.*, **43**, 2904–2911, doi:10.1002/2016GL067849.

Smy, L. A., and R. K. Scott, 2009: The influence of stratospheric potential vorticity on baroclinic instability. *Quart. J. Roy. Meteor. Soc.*, **135**, 1673–1683, doi:10.1002/qj.484.

Song, Y., and W. A. Robinson, 2004: Dynamical mechanisms for stratospheric influences on the troposphere. *J. Atmos. Sci.*, **61**, 1711–1725, doi:10.1175/1520-0469(2004)061<1711:DMFSIO>2.0.CO;2.

Tanaka, H. L., and H. Tokinaga, 2002: Baroclinic instability in high latitudes induced by polar vortex: A connection to the Arctic oscillation. *J. Atmos. Sci.*, **59**, 69–82, doi:10.1175/1520-0469(2002)059<0069:BIIHLI>2.0.CO;2.

Thompson, D. W. J., J. C. Furtado, and T. G. Shepherd, 2006: On the tropospheric response to anomalous stratospheric wave drag and radiative heating. *J. Atmos. Sci.*, **63**, 2616–2629, doi:10.1175/JAS3771.1.

Wittman, M. A. H., A. J. Charlton, and L. M. Polvani, 2007: The effect of lower stratospheric shear on baroclinic instability. *J. Atmos. Sci.*, **64**, 479–496, doi:10.1175/JAS3828.1.

Yoden, S., T. Yamaga, S. Pawson, and U. Langematz, 1999: A composite analysis of the stratospheric sudden warmings simulated in a perpetual January integration of the Berlin TSM GCM. *J. Meteor. Soc. Japan*, **77**, 431–445.